CrystEngComm

Accepted Manuscript

ROYAL SOCIETY OF CHEMISTRY

www.rsc.org/crystengcomm

TOC figure

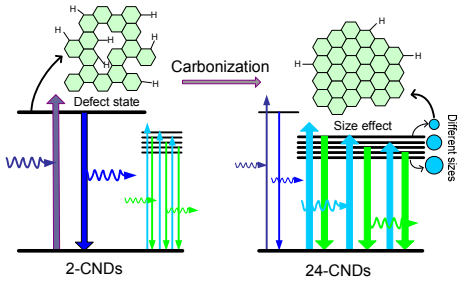

This work provides some robust evidences to support that the blue emission from carbon nano-materials arises from the carbon defects.

Cite this: DOI: 10.1039/c0xx00000x

www.rsc.org/xxxxxx

ARTICLE TYPE

Mechanism of blue photoluminescence from carbon nanodots

Zhixing Gan, Xinglong Wu,* and Yanling Hao

Received (in XXX, XXX) Xth XXXXXXXXX 20XX, Accepted Xth XXXXXXXXX 20XX
DOI: 10.1039/b000000x

The blue photoluminescence from carbon nanodots (CNDs) weakens gradually and the most intense peak red-shifts slightly as the hydrothermal reaction time increases. The 890 cm^{-1} infrared vibration band, which is associated with carbon defects, decreases with reaction time being consistent with the blue emission tendency. Based on the growth model of CNDs and understanding of photoluminescence from other carbon nano-materials, carbon defects are believed to be responsible for the blue emission.

Introduction

There has been increasing interest in carbon nanostructures such as fullerene,[1] carbon nanotubes,[2] and graphene.[3] Carbon nanodots (CNDs), an important member of the carbon family, have also attracted much attention lately.[4-25] Compared to traditional organic dyes, luminescent CNDs possess excellent biocompatibility, photo and chemical-stability, as well as tunable photoluminescence (PL).[4] Many methods such as chemical oxidation of soot,[5] laser ablation of carbon,[6,7] electrochemical oxidation of graphite,[8,9] and incomplete thermal decomposition of ammonium citrate salts[10] have been developed to prepare luminescent CNDs which have potential applications in bio-imaging,[11-14] light-emitting diodes,[15] metal ion detection,[11,16] temperature probes,[17] and intracellular pH sensing.[18] However, the lack of a thorough understanding of the PL mechanism[19] has hampered wider applications. In fact, PL from CNDs which tends to be oversimplified in many studies is excitation dependent.[8-10,13-15,17,20-24] For instance, it red-shifts as the excitation wavelength is increased. The optical properties are quite complex due to the complicated structure of CNDs including the various surface functionalities, sp^2-hybridized and sp^3-hybridized carbon, and quantum confinement effect due to the small size.[19] We have recently reported that strong blue emission at about 440 nm from reduced graphene oxide (rGO) originates from carbon defect states.[26,27] However, the situation is different in CNDs because in some cases, the PL intensity increases initially and then decreases as the excitation wavelength is changed from 340 to 480 nm, with the strongest emission being green.[9,24] In other cases, similar to the rGO, the PL intensity decreases rapidly as the excitation wavelength increases, with the blue emission being the most intense.[13-15,17,20-23] Hence, the origins of the blue and green emissions should be different but not well understood.

In this work, carbon spheres were fabricated from an aqueous glucose solution using a hydrothermal method and CNDs were collected from the supernatant.[25,28,29] The degree of carbonization was controlled by adjusting the hydrothermal reaction time. The relative intensity of the blue emission was observed to decrease gradually and the strongest PL peak red-shifted with increasing degree of carbonization. Based on analyses of the Fourier transform infrared (FTIR) spectra and carbonization mechanism, the intermediate product, organic polymers with irregular carbon rings, was believed to be the origin of the blue emission. The proposed PL mechanism is very similar to that of rGO and may be extended to other types of luminescent carbon nano-materials.

Experimental section

In the preparation, 3.96 g of glucose were dissolved in 40 mL water to form a clear solution in a 50 mL Teflon-sealed autoclave and maintained at 160 ^{o}C for 2-24 h. After 2 h, a light brown solution without precipitates was obtained. Transmission electron microscopy (TEM, JEOL, JEM-2100) and dynamic light scattering (DLS, Malvern, Zeta sizer Nano ZS) did not reveal the presence of solid particles. After reacting for 10, 16, and 24 h, precipitates were formed, collected by centrifugation, and washed thoroughly with distilled water and ethanol thrice. The precipitates and supernatant from the last centrifugation step were further characterized. Scanning electron microscopy (SEM, Hitachi, S-3400N II) confirmed the formation of carbon spheres and the CNDs in the supernatant were also characterized by TEM, DLS, and FTIR (Nicolet Nexus870). Here, the products obtained from the 2, 10, 16, and 24 h hydrothermal treatment are designated as 2-CNDs, 10-CNDs, 16-CNDs, and 24-CNDs, respectively. PL measurements were performed on an Edinburgh FLS-920 PL spectrometer. There is a kink at about 450 nm in all the obtained PL spectra and it was caused by the spectrometer.

Results and discussion

The SEM image of the 24 h carbon spheres in the precipitates in Fig. 1a shows that the carbon spheres are about 100 nm in size which is in agreement with the size distribution obtained by DLS (Fig. 1b). The diameter of the carbon spheres is influenced by the reaction time.[28] As the time is increased from 10 to 16 and then 24 h, the diameters are 60, 70, and 100 nm, respectively. Fig. 1c depicts a representative TEM image of 24-CNDs in the supernatant and the size distribution determined by DLS is shown in Fig. 1d. The average diameter of 24-CNDs is about 13 nm. Since the sizes obtained by DLS are the hydrated sizes and usually slightly larger than real sizes. Again, no dots and spheres can be found from the TEM and SEM images and no

DLS peaks can be observed from the 2 h sample. The approximate sizes of C spheres and CNDs formed at each stage are listed in Fig. 1e. The results indicate that the C spheres and CNDs appear when the reaction time is more than 2 h and the size increases with reaction time.

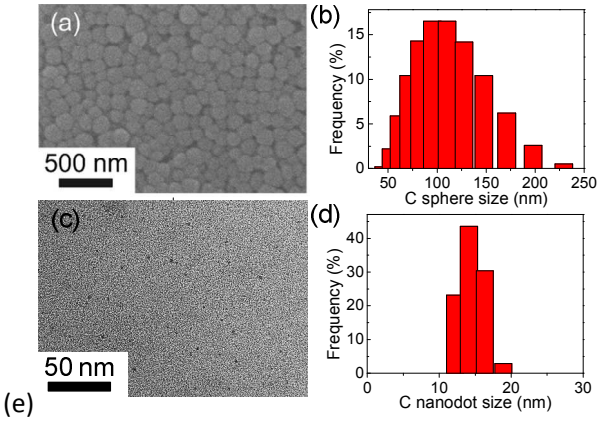

(e)

Hydrothermal time (h)	2	10	16	24
C sphere	No C sphere	60 nm	70 nm	100 nm
CND	No CND	5 nm	10 nm	13 nm

Fig. 1 (a) SEM image of the carbon spheres synthesized hydrothermally for 24 h and (b) corresponding DLS results. (c) TEM image of 24-CNDs and (d) Size distribution obtained by DLS. (e) Table for the sizes of C spheres and CNDs formed at each stage.

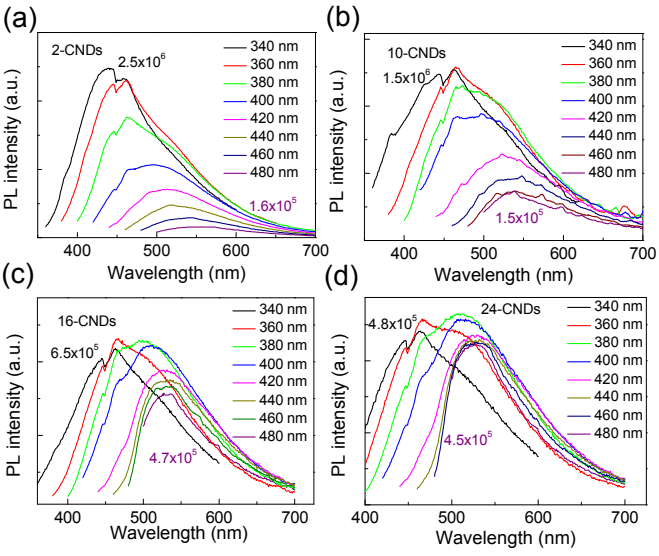

Fig. 2 (a-d) PL spectra acquired from 2-CNDs, 10-CNDs, 16-CNDs, and 24-CNDs excited by 340-480 nm light. The blue PL (excited at 340 nm) and green PL (excited at 480 nm) intensity values are shown.

Figs. 2a-d present the PL spectra acquired from 2-CNDs, 10-CNDs, 16-CNDs and 24-CNDs, respectively. As the excitation wavelength is increased from 340 to 480 nm, the emission wavelength changes from 440 to 550 nm and the blue PL (excited at 340 nm) and green PL(excited at 480 nm) intensity values are shown in each figure. As shown in Fig. 2a, the blue emission (excited at 340 nm) is much stronger than the green emission (excited at 480 nm). As shown in Figs. 2c and d, compared to the green emission, the blue emission weakens as the reaction time is increased. When the reaction time is increased to 24 h, the intensities of the blue and green emissions are almost the same. To accurately compare the blue and green emission intensities, the broad and asymmetric PL spectra excited at 340 nm are Gaussian divided into two peaks at 430 nm (EmA) and 510 nm (EmB) (Figs. 3a-d). Their changes in integral intensities [I(1), I(2)] and intensity ratio [I(1)/I(2)] with reaction time are plotted in Fig. 3e. A clear decrease in I(1) and intensity ratio can be observed, but I(2) slightly changes. Fig. 3f shows the photographs of the aqueous solutions with CNDs irradiated by a 325 nm laser (Kimmon, He-Cd laser). 2-CNDs exhibit very bright blue emission but no obvious blue emission occurs for 10-CNDs, 16-CNDs, and 24-CNDs. Hence, the decrease in PL intensity ratio mainly stems from weakening of the blue PL intensity with reaction time. Here, we should mention that the position of the most intense PL peak from the four CND solutions redshifts monotonically from 445 to 511 nm as the reaction time is increased, but the two divided subpeaks have almost the same positions. The evolution of blue emission correlates with the degree of carbonization. Since the blue emission is the strongest but no C dots and spheres form in the 2-CNDs, an intermediate product or related structure may be responsible for the blue emission. As carbonization continues, the intermediate state vanishes gradually and consequently, the blue emission weakens.

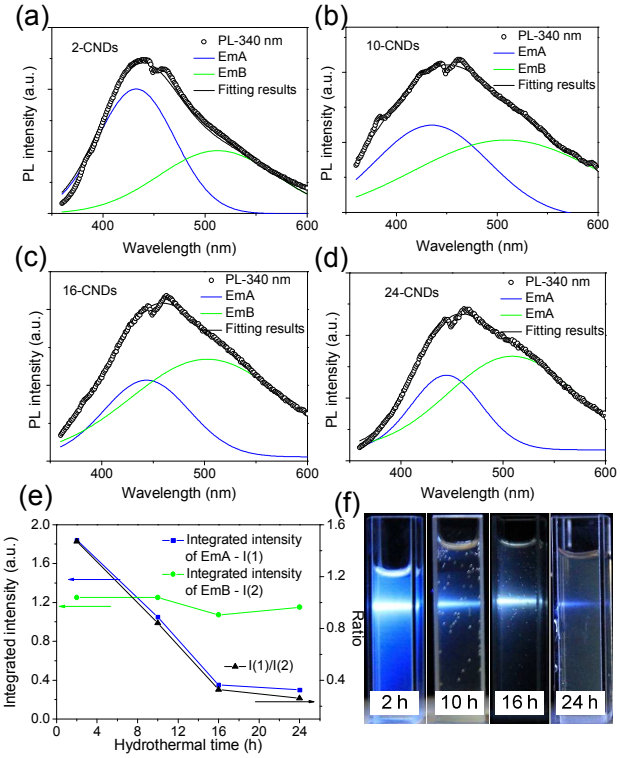

Fig. 3 (a-d) Gaussian fitting of the PL spectra obtained under excitation with the 340 nm light. EmA at 430 nm and EmB at 510 nm are fitted out. (e) Integral intensities of EmA [I(1)] and EmB [I(2)] as well as their intensity ratio [I(1)/I(2)] versus hydrothermal time. (f) Photographs of the aqueous solutions containing CNDs under irradiation by the 325 nm laser.

To study the intermediate product or structure, FTIR is performed. As shown in Fig. 4a, the vibration bands in 1000–

1300 cm^{-1} are assigned to C–OH stretching and OH bending,[28] and stretching of C–OH at 3380 cm^{-1} and C–H vibrations at 2910 and 1385 cm^{-1} are also observed,[16] implying the existence of a large number of residual hydroxyl group. The shoulder band at 1720 cm^{-1} indicates C=O vibration.[20] The intensity of the band at around 1650 cm^{-1} attributed possibly to C=C vibration increases gradually with the hydrothermal time. Appearance of this band suggests aromatization of glucose during the hydrothermal treatment. The C=C vibration is not pronounced in the 2 h sample because of the limited number of carbon frameworks formed. This is the reason why no dots can be observed by TEM but the blue emission from this sample is the most intense. The relationships between C=C and C-H vibration intensities and hydrothermal time are shown in Fig. 4b. The band at 890 cm^{-1} assigned to aromatic C-H out-of-plane bending[29] provides more information about the structural evolution. Obviously, this kind of bending should be weak in the sp^2 network with a large area such as graphite but for a carbon structure with defects or organic molecules containing irregular carbon rings, the bonding between aromatic ring and hydrogen is considerable. As shown in Fig. 4b, the intensity of the band at 890 cm^{-1} diminishes with reaction time and the trend is anti-related with the C=C vibration FTIR band, whereas the C-H vibration intensity has similar trend with the integral PL intensity ratio [I(1)/I(2)]. Hence, carbon defects or aromatic C-H vibrations may be responsible for the blue emission.

Previously, we have known that the pristine graphene oxide fabricated by Hummers method has many aromatic C-H structures, but no blue emission is detected.[27] Previous theoretical calculations also indicate that the highest occupied molecular orbital (HOMO) and lowest unoccupied molecular orbital (LUMO) of a single benzene ring passivated by hydrogen is about 7 eV.[30] Thus, the aromatic C-H cannot be responsible for the blue emission. However, our previous density functional theory simulations have confirmed that an electronic state appears in the energy range of 2.7–2.9 eV in the case with the presence of carbon defects,[27] which can cause a blue emission. Hence, the blue PL is believed to be related with carbon defects.

As reported previously,[28,29] the growth of C spheres and CNDs seems to be consistent with the LaMer model,[30] as shown schematically in Fig. 5. The glucose molecules undergo polymerization initially and when the hydrothermal time is less than 2 h, although no carbon spheres or CNDs are formed, orange or light brown solutions can be obtained, indicating that intermediate aromatic compounds and oligosaccharides are produced. These soluble organic polymers contain some complete aromatic rings (hexagons) and many incomplete (with carbon vacancy) or irregular carbon rings (pentagon, heptagon). In this stage, though no CNDs form, some carbon networks appear as confirmed by the weak infrared band at 1650 cm^{-1}. When the hydrothermal time is increased to 10 h, nucleation of CNDs begins. The macromolecules formed in the previous step, for example, linear or branchlike oligosaccharides, undergo carbonization which arises from cross-linking induced by intermolecular dehydration.[28] The resulting nuclei grow uniformly and isotropically toward the CNDs and C spheres. In this stage, the irregular carbon rings are converted into complete hexagonal rings and the sp^2 clusters are established. This is the reason why the intensity of the C = C bands in the FTIR spectra increases while that of aromatic C-H decreases as the hydrothermal time is increased. The carbonization mechanism is in good agreement with the FTIR results.

It is interesting to compare the difference of the blue emission from CNDs, graphene quantum dots (GQDs), and rGO. Firstly, the PL spectra obtained in this work are very similar to those widely observed in CNDs[6,9,10,13-17,20-22,24,25] and GQDs.[26,27,30,32-35] Secondly, the bonding structures of CNDs and GQDs are almost the same. They both contain oxygen-related groups, carbon defects, and small size sp^2 carbon clusters. Main difference is the number of carbon layers. Therefore it is expectable to have similar electronic states and PL mechanisms for these carbon nano-materials.

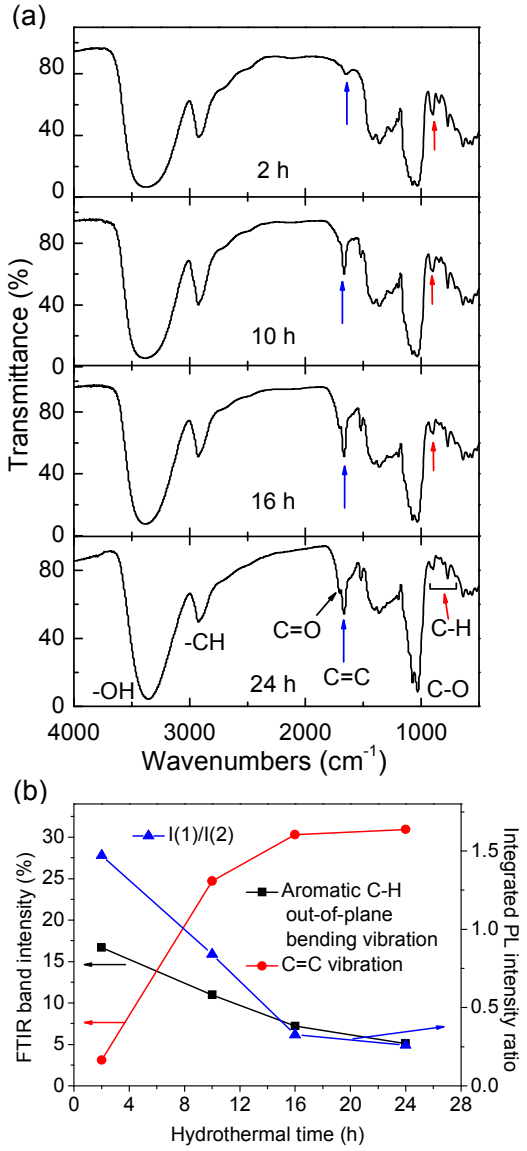

Fig. 4 (a) FTIR spectra of the hydrothermal products in the supernatants. The red arrows indicate decreasing aromatic C-H bending intensity whereas the blue arrows suggest increasing degree of carbonization. (b) Aromatic C-H (890 cm^{-1}) and C=C (1650 cm^{-1}) vibration intensities and integral PL intensity ratio [I(1)/I(2)] versus hydrothermal time. The FTIR intensity is calculated from the absolute absorbance.

Referring to PL from rGO, the strong blue emission is

related to carbon defect states formed during reduction of GO.[27] During polymerization of glucose, organic polymers with incomplete or irregular carbon rings are obtained, similar to the sp^2 cluster containing carbon defect states. They may be responsible for the blue emission. As the hydrothermal reaction proceeds, carbonization occurs and more carbon atoms are involved in the formation of the carbon networks. The number of carbon defect states is reduced and the blue emission weakens. It should be mentioned that the blue emission can always be observed regardless of the sample preparation process.[13-15,17,20-23] In most cases, no intermediate polymer is formed, but carbon defects cannot be avoided irrespective of the preparation method. Hence, the blue emission can be ascribed to carbon defect states although not all the defects in the carbon materials are fluorescent. PL activation of the carbon defect states should satisfy certain conditions. For example, the blue emission may not be possible from a small organic molecule with a single isolated irregular carbon ring. The activation conditions are still not well understood and more research is needed.

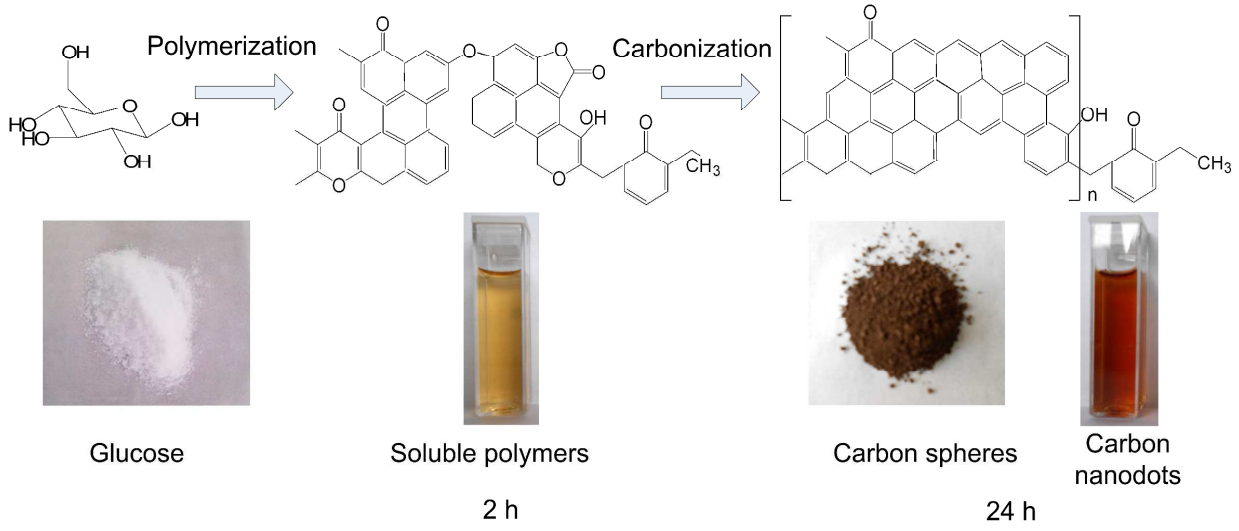

Fig. 5 Schematic model illustrating the growth of CNDs and corresponding photographs of the samples in each stage.

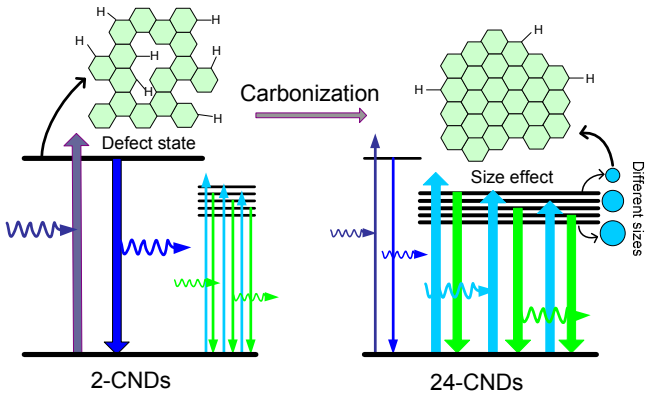

Fig. 6 Schematic illustration of the PL mechanism from CNDs. The width and thickness of the lines represent population of states and possibility of optical transition. For 2-CNDs, the PL is dominated by the blue emission, which originates from defect states (the left side). As carbonization continues, the carbon defects decreases and more sp^2 carbon clusters form. The size effect of carbon clusters becomes the dominated origin of the PL (the right side for 24-CNDs).

For GQDs or rGO, the blue emission at about 440 nm is always much stronger than the long-wavelength emission.[26,27,30,32-35] However, the situation is different in CNDs. In some cases, the PL intensity increases initially and then decreases as the excitation wavelength is changed from 340 to 480 nm, with the strongest emission being green.[9,24] In other cases, similar to rGO, the PL intensity decreases rapidly as the excitation wavelength increases, with the blue emission being the most intense.[13-15,17,20-23] For most previous investigations, GQDs were obtained by top-down process such as cutting of graphene oxide. Usually, the density of carbon defects is very high so that the PL shows strong blue emission. However, for CNDs, the fabrication methods vary with sample. In some cases, the density of carbon defects is low, thus no conspicuous blue PL peak is observed. In the case for fabricating rare bottom-up GQDs,[36] the PL is very similar to that of our 24-CNDs. The emission intensity increases firstly and then decreases as the excitation wavelength increases. The strongest emission appears at about 500 nm. This is in good agreement with our conclusion. So it is reasonable and reliable to cite the previous work[27] to support our current conclusion.

For this green emission, the surface or size effect may be a source. In 2-CQDs, no carbon dots form and so no so-called surface states exist. However, a clear redshift with increasing excitation wavelength occurs. We have known that 2-CNDs mainly contain soluble organic polymers with some sp^2 carbon clusters confirmed by our FTIR result (Fig. 4a). Thus, the size effect of sp^2 carbon clusters may cause the green emission.

Following the PL from rGO, the mechanism of PL from CNDs is illustrated in Fig. 6 with the carbon defects being responsible for the blue emission. For 2-CNDs, the density of defects is high, so the blue emission is dominant. The wavelength-dependent green emission stems from the carbon network. In other words, the size effect of the sp^2 carbon clusters causes the green PL. The energy gaps of the localized carbon network are determined by the cluster size. The smaller it is, the wider is the energy gap. The distribution of the energy gaps given

by the size distribution leads to the emissions in the range from 470 to 550 nm. The most probable size corresponds to the position of the strongest PL peak. As the degree of carbonization increases with reaction time, the density of defects decreases and more graphitic carbon clusters form. The sizes of these clusters grow up. As a result, the green emission becomes the dominated peak in the PL spectra and meantime the most intense PL peak red-shifts slightly. Here, we stress again that the strongest PL peak (blue emission) from 2-CNDs does not correspond to the most probable size of the sp^2 carbon clusters.

Conclusion

The PL from CNDs synthesized hydrothermally for different time is investigated. As the reaction time is increased, the blue emission weakens gradually and the most intense PL peak red-shifts slightly. TEM and DLS demonstrate that no CNDs are formed during 2 h hydrothermal reaction. The intensity of the C=C band in the FTIR spectra increases with reaction time and the trend is opposite to that of the blue emission. However, the intensity of the band at 890 cm^{-1} decreases with reaction time and it is consistent with the blue PL. Based on the growth model of CNDs and PL from rGO, carbon defects such as carbon vacancies and irregular carbon rings are believed to be responsible for the blue emission. The excitation wavelength-dependent green emission stems from radiative recombination of electron-hole pairs in the carbon network. This work provides some robust evidences to support such a conclusion: the carbon defects cause the blue emission from carbon nano-materials.

Acknowledgements

This work was supported by National Basic Research Programs of China under Grants Nos. 2011CB922102 and 2014CB339800. Partial support was also from National Natural Science Foundation (Nos. 21203098 and 11374141) and PAPD.

Notes and references

Nanjing National Laboratory of Microstructures and Department of Physics, Nanjing University, Nanjing 210093, P. R. China. Fax: +86 25 83595535; Tel: +86-25-83596303; E-mail: hkxlwu@nju.edu.cn

1 A. F. Hebard, M. J. Rosseinsky, R. C. Haddon, D. W. Murphy, S. H. Glarum, T. T. M. Palstra, A. P. Ramirez, and A. R. Kortan, *Nature* 1991, **350**, 600.
2 H. Baughman, A. A. Zakhidov, and W. A. de Heer, *Science* 2002, **297**, 787.
3 A. K. Geim and K. S. Novoselov, *Nat. Mater.* 2007, **6**, 183.
4 X. M. Wen, P. Yu, Y. R. Toh, Y. C. Lee, A. C. Hsu, and J. Tang, *Appl. Phys. Lett.* 2012, **101**, 163107.
5 H. P. Liu, T. Ye, and C. D. Mao, *Angew. Chem. Int. Ed.* 2007, **46**, 6473.
6 Y. P. Sun, B. Zhou, Y. Lin, W. Wang, K. A. Fernando, P. Pathak, M. J. Meziani, B. A. Harruff, X. Wang, H. Wang, P. G. Luo, H. Yang, M. E. Kose, B. Chen, L. M. Veca, and S. Y. Xie, *J. Am. Chem. Soc.* 2006, **128**, 7756.
7 L. Cao, X. Wang, M. J. Meziani, F. S. Lu, H. F. Wang, P. G. Luo, Y. Lin, B. A. Harruff, L. M. Veca, D. Murray, S. Y. Xie, and Y. P. Sun, *J. Am. Chem. Soc.* 2007, **129**, 11318.
8 Q. L. Zhao, Z. L. Zhang, B. H. Huang, J. Peng, M. Zhang, and D. W. Pang, *Chem. Commun.* 2008, **41**, 5116.
9 L. Bao, Z. L. Zhang, Z. Q. Tian, L. Zhang, C. Liu, Y. Lin, B. P. Qi, and D. W. Pang, *Adv. Mater.* 2011, **23**, 5801.
10 A. B. Bourlinos, A. Stassinopoulos, D. Anglos, R. Zboril, M. Karakassides, and E. P. Giannelis, *Small* 2008, **4**, 455.
11 A. Salinas-Castillo, M. Ariza-Avidad, C. Pritz, M. Camprubi-Robles, B. Fernandez, M. J. Ruedas-Rama, A. Megia-Fernandez, A. Lapresta-Fernandez, F. Santoyo-Gonzalez, A. Schrott-Fischer, and L. F. Capitan-Vallvey, *Chem. Commun.* 2013, **49**, 1103.
12 S. K. Bhunia, A. Saha, A. R. Maity, S. C. Ray, and N. R. Jana, *Sci. Rep.* 2013, **3**, 1473.
13 L. M. Shen, L. P. Zhang, M. L. Chen, X. W. Chen, and J. H. Wang, *Carbon* 2013, **55**, 343.
14 Z. A. Qiao, Y. F. Wang, Y. Gao, H. W. Li, T. Y. Dai, Y. L. Liu, and Q. S. Huo, *Chem. Commun.* 2010, **46**, 8812.
15 X. Guo, C. F. Wang, Z. Y.Yu, L. Chen, and S. Chen, *Chem. Commun.* 2012, **48**, 2692.
16 S. J. Zhu, Q. N. Meng, L. Wang, J. H. Zhang, Y. B. Song, H. Jin, K. Zhang, H. C. Sun, H. Y. Wang, and B. Yang, *Angew. Chem. Int. Ed.* 2013, **52**, 3953.
17 P. C. Chen, Y. N. Chen, P. C. Hsu, C. C. Shih, and H. T. Chang, *Chem. Commun.* 2013, **49**, 1639.
18 W. Shi, X. H. Li, and H. M. Ma, *Angew. Chem. Int. Ed.* 2012, **51**, 6432.
19 S. N. Baker and G. A. Baker, *Angew. Chem. Int. Ed.* 2010, 49, 6726.
20 R. L. Liu, D. Q. Wu, S. H. Liu, K. Koynov, W. Knoll, and Q. Li, *Angew. Chem. Int. Ed.* 2009, **48**, 4598.
21 C. F. Wang, X. Wu, X. P. Li, W. T. Wang, L. Z. Wang, M. Gu, and Q. Li, *J. Mater. Chem.* 2012, **22**, 15522.
22 F. Wang, S. P. Pang, L. Wang, Q. Li, M. Kreiter, and C. Y. Liu, *Chem. Mater.* 2010, **22**, 4528.
23 D. Y. Pan, J. C. Zhang, Z. Li, C. Wu, X. M. Yan, and M. H. Wu, *Chem. Commun.* 2010, **46**, 3681.
24 X. J. Mao, H. Z. Zheng, Y. J. Long, J. Du, J. Y. Hao, L. L. Wang, and D. B. Zhou, *Spectrochimica Acta Part A* 2010, **75**, 553.
25 Z. C. Yang, M. Wang, A. M. Yong, S. Y. Wong, X. H. Zhang, H. Tan, A. Y. Chang, X. Li, and J. Wang, *Chem. Commun.*2011, **47**, 11615.
26 **101**Z. X. Gan, S. J. Xiong, X. L. Wu, C. Y. He, J. C. Shen, and P. K. Chu, *Nano Lett.* 2011, **11**, 3951.
27 Z. X. Gan, S. J. Xiong, X. L. Wu, T. Xu, X. B. Zhu, X. Gan, J. H. Guo, L. T. Sun, and P. K. Chu, *Adv. Opt. Mater.* 2013, **1**, 926.
28 X. M. Sun and Y. D. Li, *Angew. Chem. Int. Ed.* 2004, **43**, 597.
29 M. Sevilla and A. B. Fuertes, *Chem. Eur. J.* 2009, **15**, 4195.
30 K. LaMer, *Ind. Eng. Chem*. 1952, **44**, 1270.
31 G. Eda, Y. Y. Lin, C. Mattevi, H. Yamaguchi, H. A. Chen, I. S. Chen, C. W. Chen, and M. Chhowalla, *Adv. Mater.* 2010, **22**, 505.
32 D. Y. Pan, J. C. Zhang, Z. Li, and M. H. Wu, *Adv. Mater.* 2010, **22**, 734.
33 M. Li, W. B. Wu, W. C. Ren, H. M. Cheng, N. J. Tang, W. Zhong, and Y. W. Du, *Appl. Phys. Lett.* 2012, **11**, 103107.
34 J. H. Shen, Y. H. Zhu, X. L. Yang, J. Zong, J. M. Zhang, and C. Z. Li, *New J. Chem.* 2012, **36**, 97.
35 Q. S. Mei, K. Zhang, G. J. Guan, B. H. Liu, S. H. Wang, and Z. P. Zhang, *Chem. Commun.* 2010, **46** , 7319.
36 R. L. Liu, D. Q. Wu, X. L. Feng, and K. Mullen, *J. Am. Chem. Soc.* 2011, **133**, 15221.

TOC figure

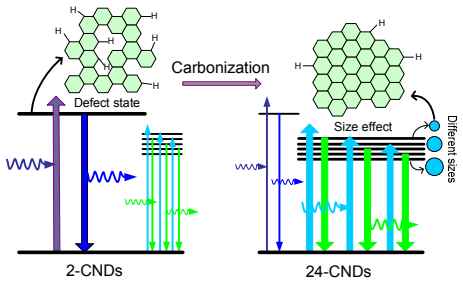

This work provides some robust evidences to support that the blue emission from carbon nano-materials arises from the carbon defects.